Spectral fluctuation properties of Hamiltonian systems: the transition region between order and chaos

1985 J. Phys. A: Math. Gen. 18 2751

(http://iopscience.iop.org/0305-4470/18/14/026)

J. Phys. A: Math. Gen. **18** (1985) 2751-2770. Printed in Great Britain

Spectral fluctuation properties of Hamiltonian systems: the transition region between order and chaos

T H Seligman†, J J M Verbaarschot and M R Zirnbauer

Max-Planck-Institut für Kernphysik and Institut für Theoretische Physik der Universität Heidelberg, West Germany

Received 2 January 1985

Abstract. We study numerically the classical dynamical behaviour, and the spectral fluctuation properties, of a class of Hamiltonian systems with two degrees of freedom. The quantum mechanical properties of these systems are monotonic but non-universal functions of the fraction of classical phase space filled by chaotic trajectories. It is found that the observed spectral fluctuation measures can be reproduced by a random-matrix model which depends on one parameter only.

1. Introduction

Classical nonlinear dynamics is a fast-growing field of current research, and considerable progress has been made in our understanding of the chaotic behaviour of maps, billiards, and other nonlinear systems. So far, dissipative systems have received most of the attention, possibly because they exhibit such intriguing phenomena as strange attractors, which do not occur in the absence of dissipation. There exists, however, a long-standing interest in conservative (or Hamiltonian) systems, too. This interest was further stimulated by the recent inquiry into manifestations of classical chaotic motion in quantum mechanics. It is by now well understood that Hamiltonian systems give rise to a very rich variety of classical dynamical behaviour, ranging from regular to completely chaotic motion. The prototype of such behaviour is found in the Henon-Heiles (1964) system, but we wish to emphasise that, actually, most non-integrable Hamiltonian systems are capable of displaying similar dynamical complexity.

It is generally agreed that the rich dynamics of Hamiltonian systems arises from the nonlinearity of the classical equations of motion. Quantum mechanics, on the other hand, is a linear theory, both in its time-dependent and time-independent forms. This has led many physicists to ask how the linearity of the Schrödinger equation can be reconciled with the observation of chaotic motion in the classical limit. We now understand that classical chaos does manifest itself in quantum mechanics, and can be associated, for example, with universal fluctuation laws governing the statistical properties of the energy levels.

Due to their invariant (or basis-independent) nature, spectral properties are particularly well suited for analysing the impact of classical chaotic motion on quantum mechanics. (Chaos in quantum mechanics can also be studied using the information

† Permanent address: Instituto de Fisica, University of Mexico in Cuernavaca (UNAM), Apdo. post. 01000 México DF, México.

0305-4470/85/142751+20$02.25

contained in eigenfunctions (see, e.g., Heller 1984, Shapiro and Goelman 1984), but one should bear in mind that this information is basis-dependent.) Bohigas *et al* (1984a) first associated chaotic behaviour in classical mechanics with fluctuation properties of the corresponding quantum system. By extending the work of Berry (1981), they showed convincingly that the statistical properties of the spectrum of Sinai's billiard can be described by a random-matrix model, namely the Gaussian orthogonal ensemble (GOE). Recently, they gave a very complete account of their work, including recent results for the stadium (Bohigas and Giannoni 1984, see also Bohigas *et al* 1984b). Another elucidating review related to these topics has been given by Berry (1983).

Due to conservation of energy, the classical motion of Hamiltonian systems with only one degree of freedom (1D systems) is integrable and therefore regular. Chaotic behaviour requires the destruction of at least one integral of motion. The simplest case where this can happen is given by 2D systems and, to date, most publications on chaoticity in Hamiltonian systems deal with this case. We should, however, be aware that due to the absence of Arnold diffusion (Chirikov 1979) in 2D systems, the phase space structure of such systems is essentially different from that of systems with three or more degrees of freedom.

The present work is concerned with the effects on quantum mechanics of the transition from order to chaos in classical 2D systems. Some preliminary results of our work have already been reported (Seligman *et al* 1984, henceforth referred to as SVZ). We base our approach on the analysis of spectral fluctuations, using the same fluctuation measures as Bohigas *et al* (1984a). The behaviour which we find for strongly chaotic systems agrees with their results. The main emphasis of our work is on spectral fluctuations in the regime intermediate between classical regular and classical chaotic motion. In SVZ the conjecture was put forth that the fraction of phase space covered by chaotic trajectories (for brevity henceforth referred to as the 'chaotic volume') is the classical order parameter controlling the change in spectral fluctuation properties. The results presented in the present paper indicate that the situation is actually more complicated. By combining a semi-classical argument with the results that are known for the regular and chaotic limiting cases, Berry and Robnik (1984) have given a closed expression describing the distribution of nearest-neighbour spacings in the transition regime. This formula is expected to be valid in the extreme semi-classical limit, but does not quite agree with our numerical data.

The purpose of this paper is to complete the work outlined in SVZ and to summarise the major results. In § 2, a family of Hamiltonian systems is studied numerically with regard to their classical dynamical behaviour. Section 3 contains our results for the spectral fluctuation properties of these Hamiltonians. A random-matrix model which reproduces the observed quantum mechanical behaviour is described in § 4, and a discussion of our results is given in § 5.

2. Classical dynamical behaviour

Numerical limitations compel us to study systems that are as simple as possible. Of course, these systems have to show the principal characteristics of chaos, and they must retain a relationship to physically meaningful models. These conditions can, e.g., be met by considering two interacting particles moving in one dimension under the influence of an external potential. The explicit form of the potentials which we have

studied is given by (the Hamiltonian being $H=\frac{1}{2}p_1^2+\frac{1}{2}p_2^2+V(x_1, x_2)$)

$$V(x_1, x_2)=V_1(x_1)+V_2(x_2)+V_{12}(|x_1-x_2|), \tag{1a}$$

with

$$V_i(x_i)=\alpha_i x_i^2+\beta_i x_i^4+\gamma_i x_i^6, \tag{1b}$$

where $i=1, 2, 12$ and $x_{12}=x_1-x_2$. By an appropriate choice of parameters, we can obtain systems that undergo a transition from integrable to strongly chaotic motion as the interaction strength λ is increased (see table 1 for the definition of λ). We have taken a polynomial form for V because this simplifies both the classical and the quantum mechanical computations. The parameters α_i, β_i and γ_i can be chosen in such a way that the potential resembles the lower part of realistic nuclear or molecular potentials. The restriction to even polynomials was made to conserve parity. In order to break the particle-exchange symmetry, we always take the potential V_1 different from the potential V_2.

Table 1. The parameters of the potential defined in equation (1). In the text the different systems are referred to by the letter in the first column.

Potential	α_1	β_1	γ_1	α_2	β_2	γ_2	α_{12}	β_{12}	γ_{12}
A	156.3	−61.0	31.8	69.4	−12.1	2.8	-100λ	25.0λ	8.3λ
B	0	122.1	0	0	24.1	0	0	-50λ	0
C	0	0	31.8	0	0	2.8	0	0	8.3λ
D	−15.6	122.1	0	−6.9	24.1	0	0	-50λ	0

When choosing the parameters of the classical system, we have to keep in mind the corresponding quantum mechanical problem. We wish to study the spectral statistics as a function of certain classical parameters such as the chaotic volume and the Kolmogorov entropy. The systems which we study must, therefore, satisfy two conditions. First, the classical parameters must remain approximately constant over a sufficiently large energy range. This constancy is needed for acquiring enough spectral statistics. Second, the classical parameters must be easy to vary. The first condition is best met by considering scale-invariant systems, i.e. systems for which solutions of the classical equations of motion on different energy shells are related by scale transformations. Scale-invariant systems result from (1) by taking the potentials V_i as homogeneous and of the same order (Landau and Lifshitz 1969). For systems with scale invariance, the chaotic volume and the Lyapunov exponent (as defined by Seligman *et al* 1985) are energy independent. As the parameter λ varies from zero to the value for which the two interacting particles dissociate, the chaotic volume typically ranges from 0 to 1.0. Systems with homogeneous potentials of fourth order (see table 1) are of special interest because of their relation to a particular limit of the classical Yang-Mills equations (Chang 1984). Another scale-invariant system which we have investigated is constructed from homogeneous potentials of sixth order. Since the restriction to homogeneous potentials would make for too narrow a choice, we have also studied a polynomial of fourth order with a weak harmonic (single particle) term. In a previous publication (svz) we studied a potential of sixth order with all α_i, β_i and γ_i different from zero. The parameters of all aforementioned potentials are

listed in table 1. We note that the short-range interaction is repulsive in each case. The reason is that, for attractive short-range interactions, no significant amount of chaos was found.

We have integrated the classical equations of motion numerically by using the subroutine MERSON from the CERN library. Based on this subroutine, we wrote a computer program that provides either a Poincaré surface of section, or the Lyapunov exponent, or the chaotic volume. In order to check the numerical accuracy, we use the condition of energy conservation. A limit of 0.1% was imposed on the energy loss in all cases.

The Lyapunov exponent was calculated by taking two nearby points in phase space and following the time evolution of their relative distance. This distance was defined as by Seligman *et al* (1985), and it was calculated during the process of numerical integration at multiples of a characteristic time of the system. Following Benettin and Strelcyn (1978), we handled the exponential divergence of the orbits by rescaling the distance whenever it had increased to 10 000 times the initial value. The fact that we use the scale-invariant definition of Seligman and Verbaarschot (1985b) for the Lyapunov exponent is important because we aim to compare different energies and different systems.

The chaotic volume μ was calculated using a scheme suggested by Noid (1984). This is a Monte Carlo method in which initial conditions are chosen at random with probability distribution given by the measure on the energy shell

$$d\mu = \delta(E - H)\, dx_1\, dx_2\, dp_1\, dp_2. \tag{2}$$

By using the above procedure for calculating the Lyapunov exponent Λ we are able, at least in principle, to decide whether a given initial condition belongs to a regular region ($\Lambda = 0$) or a chaotic region ($\Lambda > 0$). In practice, difficulties arise whenever there are many chaotic regions with a small Lyapunov exponent. In such cases, regular and chaotic orbits can only be distinguished by integrating the equations of motion for a prohibitively long time. For intermediate values of μ we were not able to decide, in about 10% of all cases and within the limited computer time, whether an orbit was regular or chaotic. Because of the systematic error resulting from this uncertainty, we were satisfied with using only 100 different initial conditions in the Monte Carlo routine. Values of the chaotic volume for the systems listed in table 1 are given in table 2. For systems A and D the value of μ is given for different energies, and the error is quoted between brackets.

We emphasise that the numerical value of the chaotic volume yields but an incomplete picture of the transition from classical regular to classical chaotic motion. For intermediate values of μ, we generally find many different chaotic regions which melt together when μ increases. The tendency to break up into many small chaotic regions for a decreasing value of μ is more pronounced for the homogeneous potentials B and C than for systems A and D. The Poincaré surfaces of section shown in figure 1 give an indication of the complexity of the structures encountered.

The Kolmogorov entropy K is given by (Lichtenberg and Lieberman 1983)

$$K = \sum_i \mu_i \Lambda_i \tag{3}$$

where the sum runs over the different chaotic regions with relative size μ_i and Lyapunov exponent Λ_i. Clearly, we obtain it from the same Monte Carlo routine that computes the chaotic volume if we run each trajectory long enough to obtain a reliable value

for the corresponding Lyapunov exponent. Since only contributions to the Kolmogorov entropy from small Lyapunov exponents are beset with sizeable errors, the uncertainty in K is mainly due to the statistical error from the random choice of initial conditions. The error in K may therefore be somewhat smaller than the error in μ. In table 2 we give the values of K for the systems A, B, C and D, with the uncertainty given in brackets.

The method used here for calculating the chaotic volume is considerably better than that of SVZ. There, only the large chaotic regions could be taken into account, and this proved inadequate even for potential A. Thus, two of the values obtained previously are wrong, and we should have 0.84 instead of 0.6, and 0.93 instead of 0.8 for the cases given in figures 1(b) and 1(c) of SVZ. Also, as we can see from table 2, the present error bars are considerably smaller.

Table 2. The chaotic volume μ and the Kolmogorov entropy K for the potentials listed in table 1. For the non-scale-invariant systems A and D we have not only varied the interaction strength λ but also the total energy.

Potential	Energy	λ	μ	K
A	100	0.1	0.00 (5)	0.00 (5)
	150	0.1	0.00 (5)	0.00 (5)
	200	0.1	0.00 (5)	0.00 (5)
	75	0.2	0.04 (2)	0.0005 (1)
	100	0.2	0.26 (5)	0.0042 (6)
	150	0.2	0.34 (5)	0.007 (1)
	200	0.2	0.15 (3)	0.0023 (6)
	50	0.3	0.04 (2)	0.0005 (1)
	75	0.3	0.81 (5)	0.027 (3)
	100	0.3	0.84 (6)	0.049 (3)
	150	0.3	0.92 (3)	0.058 (3)
	200	0.3	0.66 (4)	0.030 (1)
	50	0.4	0.84 (5)	0.044 (4)
	75	0.4	0.88 (3)	0.086 (8)
	100	0.4	0.90 (3)	0.107 (1)
	125	0.4	0.90 (3)	0.111 (6)
	150	0.4	0.96 (3)	0.105 (1)
	175	0.4	0.99 (1)	0.092 (6)
	200	0.4	0.88 (3)	0.066 (2)
	225	0.4	0.83 (4)	0.046 (4)
	100	0.5	0.98 (2)	0.151 (3)
	150	0.5	0.96 (2)	0.121 (4)
	200	0.5	0.95 (3)	0.086 (3)
	100	1.0	1.00 (1)	0.222 (1)
	150	1.0	0.95 (3)	0.189 (2)
	200	1.0	0.94 (3)	0.163 (3)
B	30	0.01	0.25 (4)	0.009 (2)
	30	0.02	0.50 (5)	0.021 (2)
	30	0.024	0.74 (5)	0.042 (4)
	30	0.03	0.84 (4)	0.067 (4)
	30	0.04	0.95 (2)	0.108 (2)
	30	0.08	0.98 (2)	0.243 (1)
	30	0.10	1.00 (1)	0.326 (1)

Table 2. (continued)

Potential	Energy	λ	μ	K
C	30	0.0017	0.28 (4)	0.007 (2)
	30	0.0025	0.63 (5)	0.020 (3)
	30	0.0035	0.79 (5)	0.042 (4)
	30	0.005	0.92 (3)	0.75 (3)
	30	0.010	0.99 (1)	0.149 (3)
	30	0.015	1.00 (1)	0.226 (1)
	30	0.020	1.00 (1)	0.284 (2)
	30	0.025	1.00 (1)	0.353 (1)
D	20	0.01	0.50 (5)	0.035 (4)
	30	0.01	0.53 (5)	0.031 (3)
	40	0.01	0.42 (5)	0.28 (4)
	20	0.015	0.86 (4)	0.078 (4)
	30	0.015	0.83 (4)	0.066 (4)
	40	0.015	0.77 (4)	0.057 (3)
	20	0.02	0.92 (3)	0.098 (3)
	30	0.02	0.91 (4)	0.072 (4)
	40	0.02	0.88 (4)	0.078 (3)
	20	0.03	0.99 (1)	0.146 (3)
	30	0.03	0.98 (2)	0.143 (3)
	40	0.03	0.94 (3)	0.127 (4)
	20	0.04	0.99 (1)	0.194 (2)
	30	0.04	0.99 (1)	0.181 (2)
	40	0.04	0.99 (1)	0.171 (4)
	20	0.05	1.00 (1)	0.246 (1)
	30	0.05	1.00 (1)	0.233 (1)
	40	0.05	1.00 (1)	0.224 (1)

3. The spectra

Although the qualitative study of classical dynamical behaviour does not require high numerical precision, in the computation of the quantum mechanical spectrum numerical accuracy is of prime importance. For the purpose of analysing spectral fluctuations, it is necessary to determine the spacings between the energy levels to within a few per cent of the local mean spacing. We must also be sure that the sequence of computed energy levels is complete, for any omission of levels would severely distort the fluctuation measures.

The eigenvalues were calculated by evaluating the matrix of the Hamiltonian in a harmonic-oscillator basis, by truncating the basis, and by diagonalising the resulting finite matrix. The maximum matrix dimension considered was 2000. Although expansion in a harmonic-oscillator basis does not yield satisfactory results in general, for the potential defined in (1) and the parameter sets listed in table 1, good convergence was obtained. (These parameters were chosen so as to give convergent results.) The selection of parameters was made by trial and error, and it is fortunate that the scale-invariant systems B and C satisfy our stringent convergence conditions.

Several independent methods were used to ascertain and check the accuracy of our results. First, we used the simple device of comparing the eigenvalues obtained

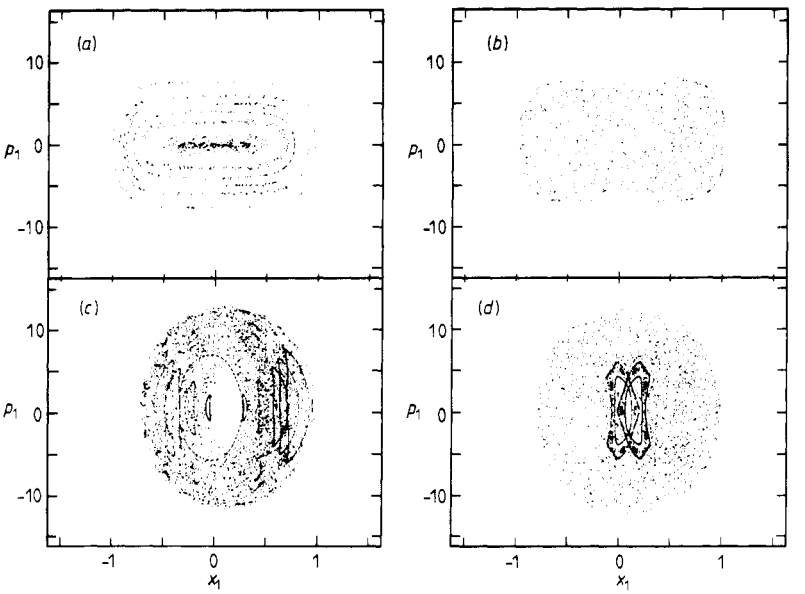

Figure 1. Poincaré surfaces of section ($p_2 = 0$) for the Hamiltonian defined in equation (1) and potentials A and C. For potential C, the interaction strengths are given by (*a*) $\lambda = 0.005$ and (*b*) $\lambda = 0.01$, and for potential D by (*c*) $\lambda = 0.3$ and (*d*) $\lambda = 0.4$. The chaotic volumes are 0.92, 0.99, 0.81 and 0.88 in (*a*), (*b*), (*c*) and (*d*), respectively.

from matrices of varying size. Second, we considered the dependence of the eigenvalues on the oscillator frequency of the basis functions. This method has been used before in the calculation of ground-state energies and we find that it can also be applied to highly excited states. Third, in specific cases we ran a computer program based on the algorithm of Neuberger and Noid (1983) to integrate the Schrödinger equation on a lattice, and compared the output with our results. (This program was adapted to the treatment of two-dimensional systems by Neuberger (1983).) Fourth, in the case of scale-invariant systems we used the observation that the eigenvalues of such systems scale with a definite power of $\hbar$. The onset of significant deviations from the predicted behaviour was found to be in rough agreement with the stability criteria defined by methods one and two. As a final test, we plotted the calculated level density as a function of energy and compared it with the semi-classical formula of Weyl. The latter was found to start deviating from our numerical results near the point where the eigenvalues become inaccurate. The consistency of all these convergence checks gives us a high level of confidence in our results. A more detailed account of the various methods used, in particular of the method of variation of the oscillator frequency for the basis functions, will be given in a separate publication (Seligman and Verbaarschot 1986).

Requiring an absolute accuracy of $0.1D$, where D is the local mean spacing, we typically obtain 400 to 500 reliable eigenvalues from matrices of dimension 1600. The following remark is important. Since it is only level spacings (and not absolute energies) that enter the calculation of fluctuation measures, one might be (mis)led to regard it as sufficient to know the *relative* position of the eigenvalues accurately, leading to weaker conditions on numerical precision (see, e.g., Noid *et al* 1977). Unfortunately,

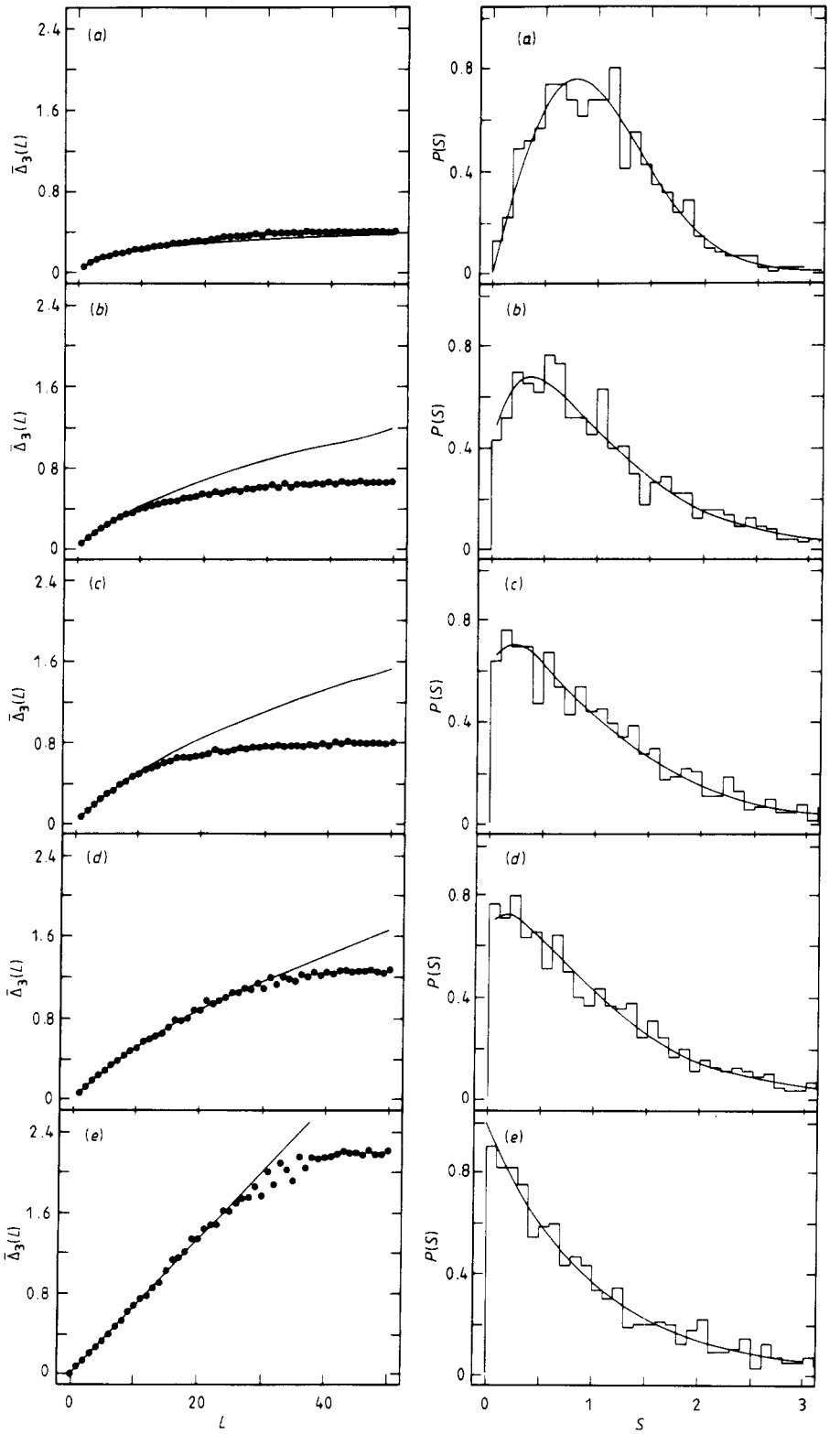
(a)
(b)
(c)
(d)
(e)
$\bar{\Delta}_3(L)$
$P(S)$
L
S

we find that the spectral properties change as soon as the *absolute* values of the eigenvalues fail to be accurate. This is rather unpleasant because for most potentials, in particular in more than two dimensions, the level density increases with energy. As a result, the requirements on accuracy become more stringent at higher energies, which is where the actual numerical accuracy decreases. It might, therefore, seem preferable to directly compute energy differences. However, the respective techniques suffer from the drawback of having a tendency to omit levels.

Having computed the spectrum, we proceed to determine its fluctuation properties via a statistical analysis. The first step is to normalise the local mean spacing to unity by 'unfolding' the spectrum. This can be done by fitting the calculated level density $\rho(E) = \Sigma_i \delta(E - E_i)$ with a sufficiently smooth function. All results given in the present paper were obtained by using

$$\rho_{\mathrm{sm}}(E) = a + b/\sqrt{E} + c/E. \tag{4}$$

(We note that the singularity at $E = 0$ on the RHS of (4) is of no consequence for our analysis because the energy of the ground state lies typically at $E > 10$.) We have also investigated other choices for ρ_{sm}, for example a polynomial of seventh order in E. In principle, it would be preferable to use the semi-classical level density for ρ_{sm} because this eliminates any bias in the fitting function, and because the semi-classical level density has a clear physical interpretation. However, on finding that all the different forms of ρ_{sm} lead to statistically equivalent results (see figure 8), we felt free to choose (4), which is most convenient numerically.

Using the smoothed level density (4), we define an unfolded spectrum by

$$\varepsilon_{i+1} - \varepsilon_i = (E_{i+1} - E_i)\,\rho_{\mathrm{sm}}(E_i). \tag{5}$$

By construction, the level spacings of the unfolded spectrum have an average value of unity. Given the ε_i, we consider two different fluctuation measures. The first measure describes short-range correlations (level repulsion) and is given by the distribution of spacings between neighbouring levels. The second fluctuation measure is the Δ_3 statistic defined by

$$\Delta_3(\alpha, L) = \min_{A,B} \frac{1}{L} \int_{\alpha}^{\alpha+L} (n(\varepsilon) - A - B\varepsilon)^2 \,\mathrm{d}\varepsilon \tag{6}$$

where $n(\varepsilon)$ denotes the number of levels in the unfolded spectrum with energy smaller than ε. The Δ_3 statistic measures long-range correlations in the spectrum. We note that, although $n(\varepsilon)$ has a slope of unity when viewed over the entire unfolded spectrum, in a subinterval $[\alpha, \alpha + L]$ this function will be best approximated by a straight line with slope different from one. A closed analytic form for expression (6) is available (Bohigas and Giannoni 1984), and we use this form to accelerate numerical computation. It is convenient to perform an energy average of Δ_3 by averaging over such values of α that the corresponding intervals overlap by $\frac{1}{2}L$ (Bohigas *et al* 1984a). We follow Bohigas *et al* (1984a) and denote the quantity so obtained by $\bar{\Delta}_3(L)$ without the additional label α.

Figure 2. Numerical results for the $\bar{\Delta}_3$ statistic and the distribution of nearest-neighbour spacings, $P(S)$. Dots and histograms represent the results obtained for the Hamiltonian (1) with potential B. The lines were obtained from a random-matrix model which is defined in § 4. Figures (*a*)-(*e*) correspond to interaction strengths $\lambda = 0.10$, 0.04, 0.02, 0.01 and 0 and chaotic volumes 1.00, 0.95, 0.50, 0.25 and 0, respectively.

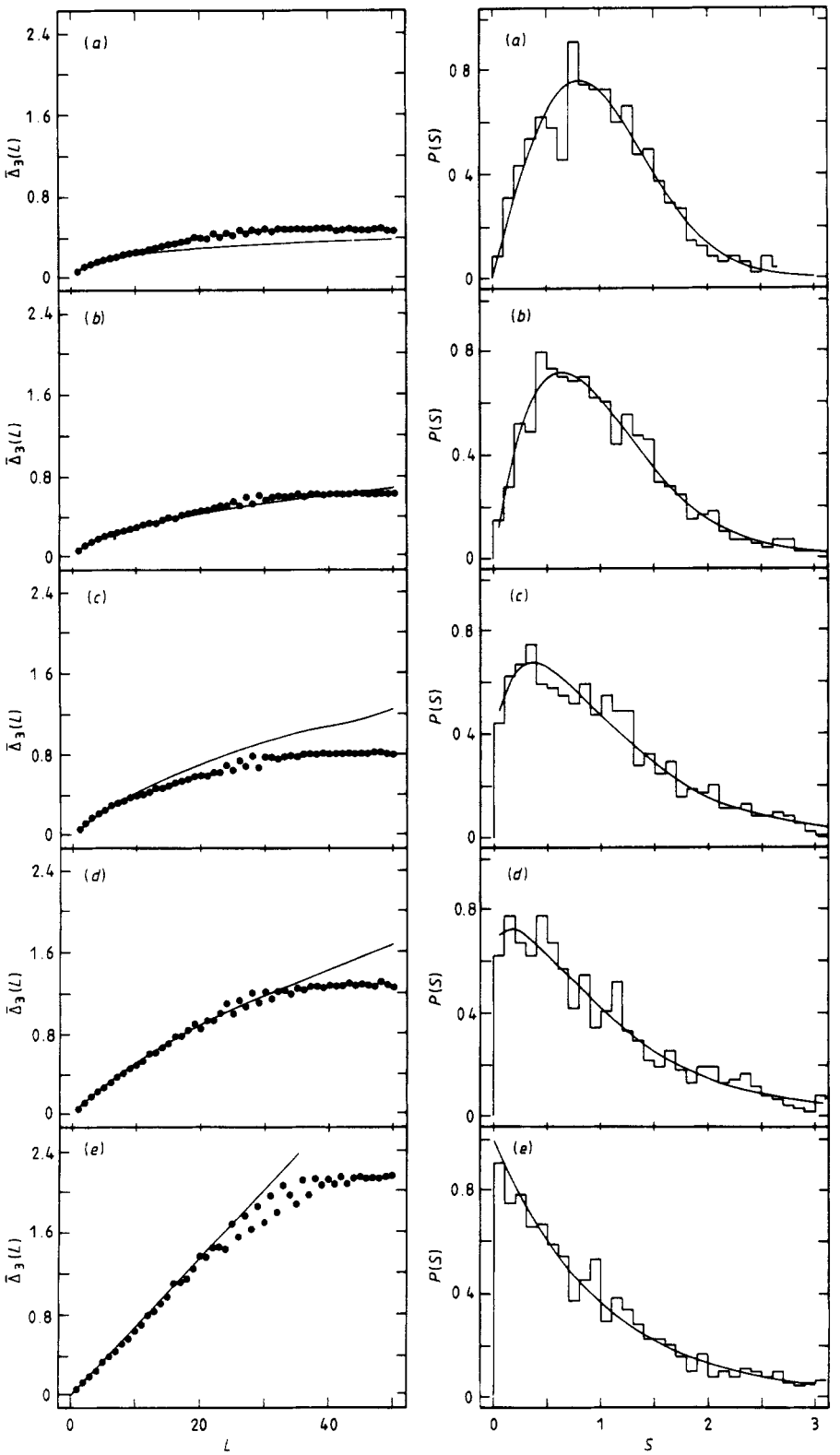
(a)
(b)
(c)
(d)
(e)
$\bar{\Delta}_3(L)$
$P(S)$
L
S

Since the spectral properties of Hamiltonian systems vary, in general, with energy, it is necessary to check whether the fluctuation measures are stationary within the spectrum span considered. We check stationarity by dividing a sequence of 450 levels, say, into three different subsequences of 150 levels each, and by calculating the distribution of nearest-neighbour spacings and the $\bar{\Delta}_3$ statistic for each subsequence separately. (A meaningful statistical analysis requires a minimum of 100 levels.) The fluctuation properties are said to be stationary when the different results obtained in this way agree within statistical errors. At this point we want to mention that for the non-scale-invariant potentials A and D we have chosen the value of $\hbar$ such that the classical properties of the system remain approximately constant over the part of the spectrum to be investigated. For the potentials A and D this amounts to a value of $\hbar$ of 0.4472 and 0.1414, respectively. For the scale-invariant systems B and C the value of $\hbar$ is irrelevant and we fix its value at 0.2.

For reasons to be discussed later, we omit the first 50 levels of each spectrum, and we combine levels with even and odd parity to form one large ensemble of about 700 to 900 levels. Figures 2, 3 and 4 show the results for the potentials B, C and D. The interaction strength decreased from top to bottom in each of the figures. The histograms on the RHS give the results for the distribution of nearest-neighbour spacings, $P(S)$. We chose to represent these results by using a bin size of 0.1, which is consistent with the accuracy of the calculated energy levels. The dots on the LHS give our results for the $\bar{\Delta}_3$ statistic. The full lines in the top graphs (a) of each figure represent the GOE predictions for $\bar{\Delta}_3$ and $P(S)$ (see § 4), and the graphs (e) at the bottom represent the predictions of the Poisson ensemble. This latter ensemble is defined by assuming the energy levels to be distributed randomly. The full lines in the graphs labelled (b), (c) and (d) are obtained from a random-matrix model which will be described in § 4.

We observe that in all three cases there is a smooth transition from the GOE limit to a behaviour that closely resembles the Poisson limit. Poisson statistics is clearly attained for the distribution of nearest-neighbour spacings, and also for the $\bar{\Delta}_3$ statistic, at least up to $L \approx 30$. These results agree with those for the potential A given in SVZ.

In the graphs (e), the most conspicuous deviation from Poisson behaviour is the 'kink' in the $\bar{\Delta}_3$ statistic, which fades as we approach the GOE limit. $\bar{\Delta}_3$ displays a marked flattening at about 30 level spacings, thereby indicating that our family of Hamiltonians yields, in the integrable limit, long-range fluctuations that are considerably smaller than those predicted by Poisson statistics. In order to understand this feature, we have considered model spectra such as

$$E_{mn} = a_1 m + b_1 m^2 + a_2 n + b_2 n^2. \tag{7}$$

(Clearly, the analysis of the corresponding spectral statistics defines a problem in number theory.) Numerical computation of $\bar{\Delta}_3$ for the spectra (7) yields a behaviour (see figure 5) quite similar to that seen in figures 2(e), 3(e) and 4(e). Furthermore, the 'kink' moves to larger values of L as the number of levels between zero and the lowest level of the part of the spectrum used for the calculation of $\bar{\Delta}_3$ is increased, which is also what we find for the numerical data given in figure 6. For the potential considered in SVZ, the 'kink' in Δ_3 occurs at much smaller values of L, $L \leqslant 9$. We interpret this as a non-generic behaviour owing to the fact that this potential contains

Figure 3. As figure 2 but with potential B replaced by potential C. The interaction strengths are given by $\lambda = 0.025$, 0.015, 0.010, 0.0035 and 0, and the chaotic volumes by 1.00, 1.00, 0.99, 0.79 and 0.

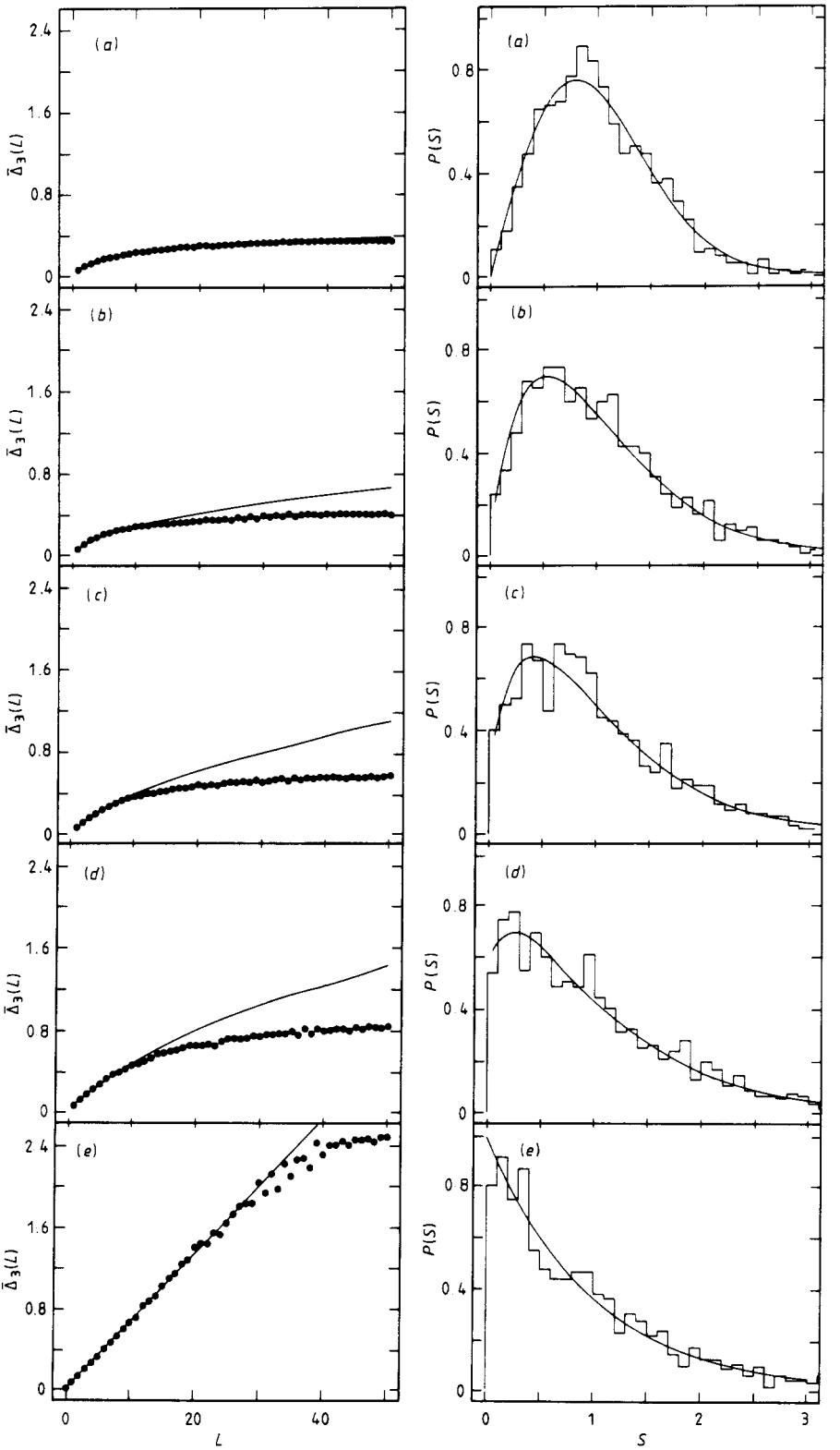
(a)
(b)
(c)
(d)
(e)
$\bar{\Delta}_3(L)$
$P(S)$
L
S

strong harmonic terms. This interpretation is consistent with figure 5(*b*) where we show for the spectrum obtained from equation (7) with $a_1 = 1.0$, $a_2 = 1.4142$, $b_1 = 1.0 \times 10^{-3}$ and $b_2 = 1.0 \times 10^{-3}$. The 'kink' shows up at much smaller values of L than in figure 5(*a*) where the harmonic term is zero. The case $a_1 = a_2 = 0$ has been studied extensively by Casati *et al* (1984a, b), and their findings are in keeping with our results. Concerning figures 2, 3 and 4 we wish to draw attention to the saw-tooth-like fluctuations of $\bar{\Delta}_3$ which may occur just before the 'kink'. This phenomenon is not an artefact of the unfolding procedure and could not be explained properly.

We have mentioned earlier that the family of Hamiltonians (1) does not give rise to stationary ensembles, in general. The above discussion suggests that problems due to non-stationarity are particularly pressing in the integrable limit. There exists firm evidence that the distance from the ground state has a significant influence on the $\bar{\Delta}_3$ statistic. To illustrate this we show in figure 6 the $\bar{\Delta}_3$ and the nearest-neighbour spacing distribution of the first 125 levels (figure 6(*a*)) and of the second 125 levels (figure 6(*b*)) for the scale-invariant system C with $\lambda = 0.01$. One sees that the 'kink' in $\bar{\Delta}_3$ moves to the right. However, the nearest-neighbour spacing distribution remains unaffected within statistical fluctuations. This is the reason why we always discard the first 50 levels from our analysis.

Since classical dynamical behaviour and quantum level fluctuations are expected to parallel each other, we put states with even and odd parity into the same ensemble. Figure 7 shows the $\bar{\Delta}_3$ statistic separately for even and odd parity in two selected cases. We were surprised to find a small yet noticeable systematic difference, which actually increases as the integrable limit is approached. At short range, even-parity states give rise to a somewhat stiffer spectrum than odd-parity states do, while at long range the situation is reversed. We have not been able to find a satisfactory explanation of this phenomenon. In any case, the differences are so small that we regard their influence as negligible as far as our main results are concerned.

Finally, we wish to substantiate our claim that we obtain results essentially equivalent to those given in figures 2, 3 and 4 when we use the semi-classical level density

$$\rho_{\mathrm{sm}}(E) = \frac{1}{2\pi\hbar^2} \int \delta(E - H)\, \mathrm{d}x_1\, \mathrm{d}x_2\, \mathrm{d}p_2\, \mathrm{d}p_2 \tag{8}$$

instead of equation (4). Results obtained from the two different forms of ρ_{sm} are compared in figure 8.

4. A random-matrix model

In the previous section we saw a gradual transition from the spectral statistics of the GOE to that of the Poisson ensemble as the chaotic volume changed from to 1.0 to 0. In this section we discuss in some detail a random-matrix model which was proposed in SVZ. This model reproduces the observed behaviour. It is also capable of predicting quantities other than the $\bar{\Delta}_3$ statistic and the distribution of nearest-neighbour spacings.

Figure 4. Same as figure 2 but with potential B replaced by potential D. The interaction strengths are given by $\lambda = 0.05$, 0.04, 0.03, 0.015 and 0, and the chaotic volumes by 1.00, 0.99, 0.97, 0.82 and 0.

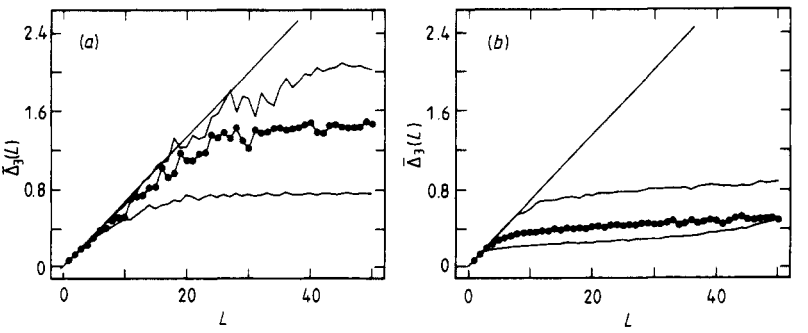

Figure 5. The $\bar{\Delta}_3$ statistic for spectra generated from equation (7) with (*a*) $a_1 = 0$, $b_1 = 1.0$, $a_2 = 0$ and $b_2 = 1.4142$, and with (*b*) $a_1 = 1.0$, $b_1 = 1.0 \times 10^{-3}$, $a_2 = 1.4142$ and $b_2 = 1.0 \times 10^{-3}$. The lower line corresponds to the first 150 eigenvalues, the dotted line to the second 150 eigenvalues, and the upper line to the 301st eigenvalue up to the 450th eigenvalue. We note that the harmonic term shifts the position of the 'kink' to lower values of L. For eigenvalue sequences higher up in the spectrum the 'kink' moves to the right.

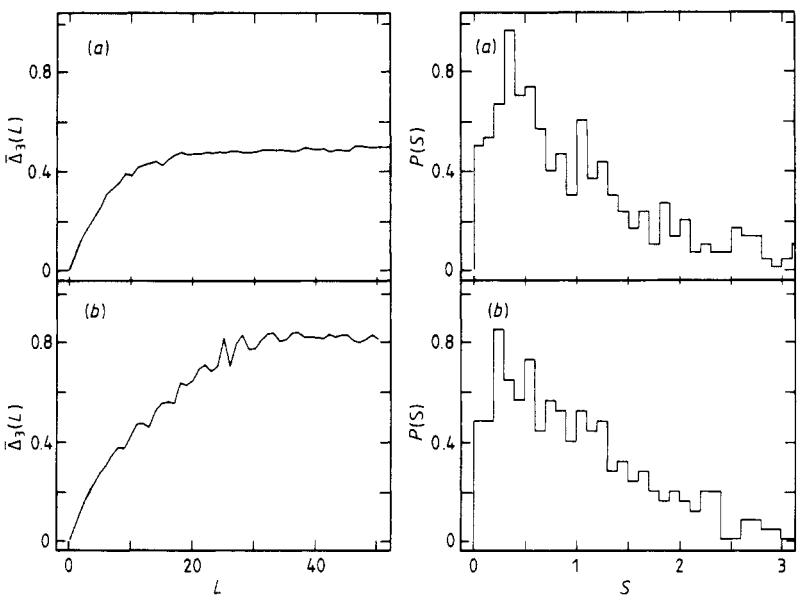

Figure 6. The $\bar{\Delta}_3$ statistic and the nearest-neighbour spacing distribution $P(S)$ for (*a*) the first 125 eigenvalues and (*b*) the second 125 eigenvalues of the potential C with strength $\lambda = 0.01$.

(We hope to investigate in the future quantities involving the spectral three- and four-point functions in order to test these predictions.)

Let X_{ij} be the matrix elements of an ensemble of GOE matrices. We then define matrix elements Y_{ij} by

$$Y_{ij} = X_{ij} \exp[-(|i-j|/\sigma)^{\kappa}]. \tag{9}$$

Due to the exponential cut-off, which is characterised by the value of κ, these matrix elements effectively describe an ensemble of 'banded' matrices, with effective band

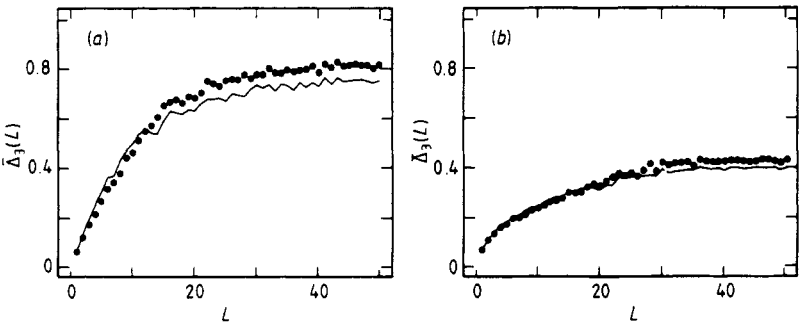

Figure 7. Comparison between levels with even parity (dots) and levels with odd parity (lines) of the $\bar{\Delta}_3$ statistic and the distribution of nearest-neighbour spacings, $P(S)$. These results were obtained from the Hamiltonian (1) with potential C and interaction strengths (*a*) $\lambda = 0.03$ and (*b*) $\lambda = 0.08$.

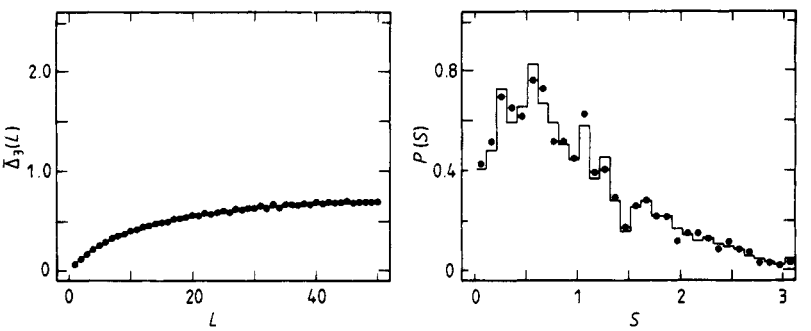

Figure 8. Comparison of the spectral statistics obtained by unfolding the calculated level density in two different ways. The full lines represent the results obtained by using the semi-classical level density, and the dots were obtained by making a χ^2 fit using the ρ_{sm} defined in equation (4). These results correspond to the Hamiltonian (1) with potential B and interaction strength $\lambda = 0.04$. In (*a*), we show the $\bar{\Delta}_3$ statistic, and in (*b*) the nearest-neighbour spacing distribution, $P(S)$.

width σ. In SVZ the value $\kappa = 2$ was used. Actually, the dependence on κ is very weak for values of $\kappa \geqslant 2$. The $\bar{\Delta}_3$ and the nearest-neighbour spacing distribution for $\kappa = 2$ and $\kappa = 4$ coincide. We arrived at this conclusion by comparing results obtained by averaging over an ensemble of 250 160×160 matrices for different values of σ. The curves for $\kappa = 1$ and $\kappa = 2$ are not identical, but by adjusting the value of σ we can obtain practically the same result. This is shown in figure 9 where we give the $\bar{\Delta}_3$ statistic for $\kappa = 1$ and $\sigma = 4$ (dots), and for $\kappa = 2$ and $\sigma = 6$ (line). These results were also obtained from an ensemble of 250 matrices of dimension 160. When σ differs from 0 and ∞, the results for $\bar{\Delta}_3$ and the nearest-neighbour spacing distribution depend on the dimensionality N of the matrices. This dependence, too, can be simulated by changing σ in an appropriate way. For definiteness we will always take $N = 160$. Of course, the argument L of $\bar{\Delta}_3(L)$ has to be well below N.

Our random-matrix model thus reduces to a single-parameter family, and this is desirable as our numerical results indicate that the spectral statistics depends only on *one* parameter.

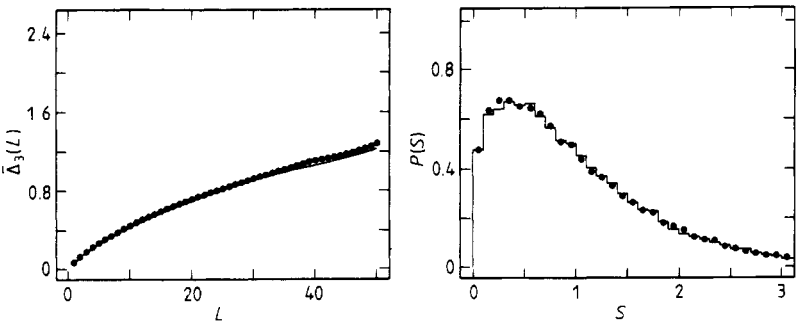

Figure 9. The $\bar{\Delta}_3$ statistic for the eigenvalues of the model defined in § 4 and different values of κ. The statistic for $\kappa = 1$ and $\sigma = 4$ (dots) is compared with the $\bar{\Delta}_3$ statistic for $\kappa = 2$ and $\sigma = 6$ (full line).

We now proceed to adjust the value of σ to the data which we have available. The curves in figures 2, 3 and 4 are obtained from an ensemble of 250 matrices with the value of σ fitted to the results for $\bar{\Delta}_3$. When the system showed an excessive stiffness at long range, as is for example the case in figure 4(c), we restricted the fit to the points below the 'kink'. The curves for the nearest-neighbour spacing distribution were calculated from the same value of σ without further adjustment. All these curves were obtained numerically by taking not only the ensemble average but also an energy average to improve the statistics. In order to further reduce the statistical errors, we smoothed the random-matrix results for $\bar{\Delta}_3(L)$ as a function of L. For the nearest-neighbour spacing distributions of the random-matrix model, the additional smoothing was applied to the data points defined by a histogram with bin size 0.1. (Note that this is the same bin size as was used in § 3.) The resulting points are interpolated by a smooth curve. The curves for the nearest-neighbour spacing distribution obtained in this way are not exact, but they represent a good approximation. By taking a resolution finer than 0.1, one finds that the spacing distribution always goes to zero at the origin (except for the Poisson limit). This feature, which is also present in the nearest-neighbour spacing distributions of figures 2, 3 and 4, cannot be explained by the semi-classical arguments of Berry and Robnik (1984). We consider this as a confirmation of the strength of our model.

Up to the 'kink' in $\bar{\Delta}_3$, the model is always in very good agreement with our data. The nearest-neighbour spacing distribution is reproduced completely within statistical fluctuations. To say it again, the results of our random-matrix model depend on one parameter only. The success of the model can therefore be taken as evidence confirming the conclusion drawn in § 3, namely that the transition from GOE to Poisson behaviour is universal in the energy range considered in this paper.

5. Discussion

Based on preliminary studies (svz) of a one-parameter family of Hamiltonians, we proposed that the chaotic volume may be the classical order parameter governing the transition of spectral fluctuation properties in quantum mechanics. Using the results given in the present paper, we are now able to put this proposition to a test. We have seen that our quantum mechanical results can be described essentially by one parameter,

and we may choose it model independently as $\bar{\Delta}_3(2) - \bar{\Delta}_3(1)$. (For obvious reasons we propose to give this quantity the following name: 'spectral order parameter'.) Plotting the spectral order parameter against the chaotic volume for all four potentials and varying interaction strength, we do not find the same behaviour in all cases (see figure 10: for the potentials A and D we have averaged the chaotic volume μ over the energy interval covered by the eigenvalues used for the calculation of the $\bar{\Delta}_3$). To be sure, the gross behaviour is independent of the system, but the detailed functional form does depend on it. The differences are significant because the functions shown in figure 10 have regions of very large and very small derivatives, amounting to a large sensitivity. The general trend, and the monotonicity of the function for each system, shows that the chaotic volume does play an important role. However, the functional dependence of the spectral fluctuation measures on this parameter is not universal.

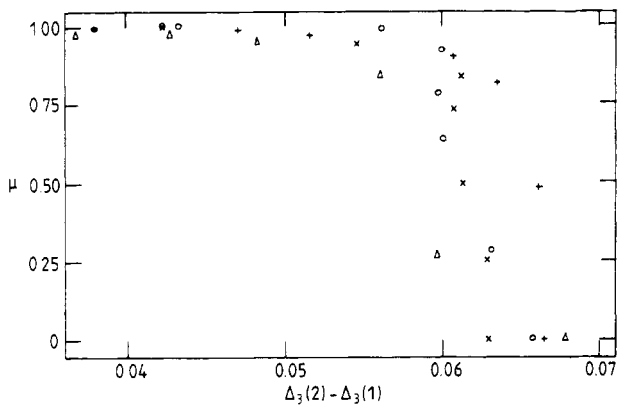

Figure 10. The chaotic volume against the spectral order parameter $\bar{\Delta}_3(2) - \bar{\Delta}_3(1)$ for the Hamiltonian (1) and the various potentials given in table 1. The results for potentials A through D are represented by △, ×, ○ and + symbols, in this order.

It is worth mentioning, here, that the Kolmogorov entropy has also been proposed as a relevant parameter for the present problem (Zaslavsky 1981). This proposition is largely refuted by our numerical data. Strongly chaotic systems are in general characterised by different values of the Kolmogorov entropy, but the corresponding spectral fluctuation measures which we obtain are universally given by the GOE. Hence, if the Kolmogorov entropy has any influence at all, then this influence must disappear in the strongly chaotic limit.

We resume the discussion of figure 10 and recall that both the distribution of nearest-neighbour spacings and the short-range part of the $\bar{\Delta}_3$ statistic are well described by a one-parameter family of curves. As is seen from figure 10, a given member of this family does not, in general, correspond to a unique value of the chaotic volume. This non-uniqueness (or non-universality) arises from differences in the classical dynamical behaviour that are not contained in the value of μ. At the end of § 2, we saw that, as the interaction strength and, consequently, the chaotic volume is reduced, the chaotic region breaks up into many disjoint pieces. This breakup occurs in a different way for each potential. Consider values of the chaotic volume between 0.9 and 1.0, where the biggest change in spectral statistics occurs. Our results show that the 'disintegration'

of the chaotic region has the effect of reducing the quantum mechanical consequences of chaos. In other words, for a fixed value of the chaotic volume, we find that the spectral statistics is closer to Poisson (or further away from GOE) when phase space contains many small instead of one large chaotic region.

This observation is consistent with the general line of reasoning used by Berry and Robnik (1984) in their derivation of a closed formula for the nearest-neighbour spacing distribution in the semi-classical limit. There exists, however, a clear difference between this formula and our numerical results. We find that the disintegration of phase space into many small chaotic regions simulates a decrease in chaotic volume, that is to say, it simply shifts the peak of the distribution closer to the origin without generating a new shape. Berry and Robnik predict also a change in shape. This difference does not imply a contradiction as the formula of Berry and Robnik (1984) is supposed to be valid only in the semi-classical limit. (A more detailed comparison between their formula and its extension to the $\bar{\Delta}_3$ statistic and our numerical results will be given elsewhere by Seligman and Verbaarschot (1985a.) We conclude that effects of quantal diffusion are important and that the main assumption made by Berry and Robnik (1984), namely that wavefunctions are localised either in a particular regular or in a particular chaotic region of phase space, is not completely valid in the energy range which we consider.

In summary, two major results have emerged from our work. First, we have seen that for the class of Hamiltonians (1), the spectral fluctuation properties at low energy exhibit a unique (or 'universal') transition behaviour from GOE to Poisson-like statistics. This transition parallels the transition from chaotic to regular motion in the corresponding classical system. The classical dynamical behaviour has a richer structure which appears, however, to be washed out by quantum fluctuations. The quantum mechanical behaviour can be described by a one-parameter random-matrix model, with an additional stiffness imposed at long range in the spectrum. This stiffness manifests itself as a 'kink' in $\bar{\Delta}_3$ which gradually fades as we approach the GOE limit. We believe it to be a general property of integrable systems with two (or few) degrees of freedom.

Second, our results provide a further link in a chain of arguments, mainly numerical in nature, which aim to establish that spectral statistics provides a key to the understanding of chaos in quantum mechanics, and that random-matrix models are the mould in which this key is formed. The chain of arguments begins with the paper of Berry and Tabor (1977) who proposed a Poisson distribution for the nearest-neighbour spacings of generic integrable systems. Berry (1981) later suggested a Wigner distribution (GOE) for the spacings of strongly chaotic (K)systems. Bohigas *et al* (1984b) showed the latter conjecture to be true for two types of billiard, namely Sinai's billiard and the stadium. Two of us (Seligman and Verbaarschot 1985b) have supplemented potentials of the type D with a magnetic field of intermediate strength to obtain spectral fluctuation measures that correspond to the Gaussian unitary ensemble (GUE). Finally, SVZ and the present paper constitute an attempt to fill in the gap between the integrable and completely chaotic limits.

An important further step will be the analysis of systems with three degrees of freedom. Arnold diffusion is expected to modify the classical picture drastically, there, and it will be interesting to see to what extent this induces changes in quantum mechanics. In particular, the role of the chaotic volume will have to be reconsidered, and also the anomalies in the integrable case should disappear with an increasing number of degrees of freedom. Unfortunately, the numerical effort will grow considerably, as was explained in § 3.

Finally, we wish to comment on a recent paper by Casati *et al* (1984a) who considered the square well in two dimensions. Their results for the $\bar{\Delta}_3$ statistic are very similar to those which we obtain in the integrable case, including the excessive long-range stiffness as expressed by the 'kink'. In addition, for the nearest-neighbour spacings they find that fluctuations about the Poisson distribution do not decrease with an increasing number of levels. This finding casts some doubt on the justification of any statistical analysis in this case. Yet, as the authors admit, the square well is a very special system. Anomalies for the harmonic oscillator are well known (Berry and Tabor 1977), and there is no reason to expect that the square well is any nearer to the generic case. A more extensive study of our systems might provide some insight. Since our systems are separable in the integrable limit, we would have to compute the spectra for the two one-dimensional systems separately, and then construct the spectrum of the total system by superposition.

Acknowledgments

We would like to thank O Bohigas, M J Giannoni and H A Weidenmüller for many useful discussions. One of us (THS) is a Fellow of the Alexander von Humboldt Foundation.

Note added in proof. In a beautiful argument Berry (1985) explains the connection between the Δ_3 statistic and the properties of the periodic classical trajectories. Among others this enabled him to explain the 'kink' in the Δ_3 statistic and the asymptotic logarithmic dependence of L of $\Delta_3(L)$ for completely chaotic systems.

References

Benettin G and Strelcyn J M 1978 *Phys. Rev.* A **17** 773
Berry M V 1981 *Ann. Phys., NY* **131** 163
—— 1983 in *Chaotic Behaviour of Deterministic Systems, Les Houches, Summer School Lectures XXXVI* ed R H G Helleman and G Joos (Amsterdam: North-Holland)
—— 1985 *Proc. R. Soc.* to be published
Berry M V and Robnik M 1984 *J. Phys. A: Math. Gen.* **17** 2413
Berry M V and Tabor M 1977 *Proc. R. Soc.* A **356** 375
Bohigas O and Giannoni M J 1984 *Lectures delivered at Workshop on Mathematical and Computational Methods in Nuclear Physics* (Berlin: Springer)
Bohigas O, Giannoni M J and Schmit C 1984a *Phys. Rev. Lett.* **52** 1
—— 1984b *J. Physique Lett.* to be published
Casati G, Chirikov B V and Guarneri I 1984a *Phys. Rev. Lett.* **54** 1350
Casati G, Guarneri I and Valz-Gris F 1984b *Phys. Rev.* A **30** 1586
Chang S 1984 *Phys. Rev.* D **29** 259
Chirikov B V 1979 *Phys. Rep.* **52** 263
Henon M and Heiles C 1984 *Astron. J.* **69** 73
Heller E J 1984 *Phys. Rev. Lett.* **53** 1515
Landau L and Lifshitz E M 1969 *Mechanics* 2nd edn (Oxford: Pergamon)
Lichtenberg A J and Lieberman M A 1983 *Regular and Stochastic Motion* (Berlin: Springer)
Neuberger B 1983 Private communication
Neuberger J W and Noid D W 1983 *Preprint* Oak Ridge National Laboratory
Noid D W 1984 Private communication
Noid D W, Koszykowski M L and Marcus M A 1977 *J. Chem. Phys.* **67** 404

Seligman T H and Verbaarschot J J M 1985a *J. Phys. A: Math. Gen.* **18** 2227
—— 1985b *Phys. Lett.* **108A**
—— 1986 to be published
Seligman T H, Verbaarschot J J M and Zirnbauer M R 1984 *Phys. Rev. Lett.* **53** 215
—— 1985 *Phys. Lett.* in press
Shapiro M and Goelman G 1984 *Phys. Rev. Lett.* **53** 1714
Zaslavsky G M 1981 *Phys. Rep.* **52** 263